

AperTO - Archivio Istituzionale Open Access dell'Università di Torino

**MRI Visualization of Melanoma Cells by Targeting Overexpressed Sialic Acid with a GdIII-dota-en-pba Imaging Reporter**

**This is the author's manuscript**

*Original Citation:*

*Availability:*

This version is available <http://hdl.handle.net/2318/140429> since

*Published version:*

DOI:10.1002/anie.201207131

*Terms of use:*

Open Access

Anyone can freely access the full text of works made available as "Open Access". Works made available under a Creative Commons license can be used according to the terms and conditions of said license. Use of all other works requires consent of the right holder (author or publisher) if not exempted from copyright protection by the applicable law.

(Article begins on next page)



# UNIVERSITÀ DEGLI STUDI DI TORINO

This is the accepted version of the following article:

Simonetta Geninatti Crich, Diego Alberti, Ibolya Szabo, Silvio Aime, Kristina Djanashvili,  
“MRI Visualization of Melanoma Cells by Targeting Overexpressed Sialic Acid with a  
Gd(III)-DOTA-EN-Phenylboronate Imaging Reporter”,  
Angew. Chem. Int. Ed. 2013, 52, 1161-1164

which has been published in final form at

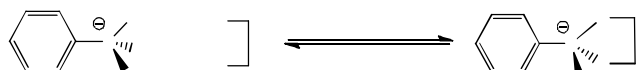
*<http://onlinelibrary.wiley.com/doi/10.1002/anie.201207131/abstract>*

# MRI Visualization of Melanoma Cells by Targeting Overexpressed Sialic Acid with a Gd(III)-DOTA-EN-Phenylboronate Imaging Reporter\*\*

Simonetta Geninatti Crich\*, Diego Alberti, Ibolya Szabo, Silvio Aime, Kristina Djanashvili\*

Altered glycosylation of cell surface proteins and lipids is frequently associated with tumorigenic and metastatic processes.<sup>[1]</sup> These changes in glycosylation are mainly caused by an increased expression of sialyltransferases, which glycosylate exposed glycans at their terminal positions with anionic monosaccharide sialic acid residues (Sia). Tumor cells overexpressing Sia appear protected to the immune defense system, and as a result, malignancy is increased.<sup>[2]</sup> Numerous studies have demonstrated that Sia are relevant biomarkers of metastatic activity of tumors,<sup>[3]</sup> and that Sia expression on cancer cells correlates with the prognosis of patients.<sup>[4]</sup> Currently the determination of the sialylation status of solid tumors is carried out on tissue sections from biopsies. This is not only an invasive procedure, it also bears an intrinsic risk that the sample is not representative for the whole, potentially heterogeneous tumor. Therefore, we have investigated probes that are able to non-invasively visualize Sia *in vivo*.

Macrocyclic or linear lanthanide complexes appear interesting candidates for this intended application, because they can be used either as contrast agents (CA) for magnetic resonance imaging (MRI) or as radiopharmaceuticals for imaging and therapy of tumors. For both tasks, accurate delivery and retention of the complex at the site of disease is mandatory. Previously, we have demonstrated the affinity of <sup>160</sup>Tb-DTPA-bisamide (DTPA = diethylenetriamine pentaacetic acid) conjugated to a phenylboronic acid (PBA) moiety towards human glioma cells.<sup>[5a]</sup> The recognition mechanism



**Scheme 1.** Formation of the 5- and 6- membered ring esters between 1,2- or 1,3 diols and phenylboronic acid at physiological pH.

[\*] Dr. S. Geninatti Crich, D. Alberti, I. Szabo, Prof. S. Aime  
Department of Chemistry, Molecular Imaging Center  
Via Nizza 52, 10126 Turin, Italy  
Fax: (+39) 01 16706487  
E-mail: [simonetta.geninatti@unito.it](mailto:simonetta.geninatti@unito.it)

Dr. K. Djanashvili  
Department of Biotechnology, Delft University of Technology  
Julianalaan 136, 2628 BL, Delft, the Netherlands  
Fax: (+31) 15 2781415  
E-mail: [k.djanashvili@tudelft.nl](mailto:k.djanashvili@tudelft.nl)

[\*\*] This research was performed in the framework of the EU COST Action TD1004, "Theranostics Imaging and Therapy: an Action to Develop Novel Nanosized Systems for Imaging-Guided Drug Delivery", and supported by Regione Piemonte (PIIMDMT and nano-IGT projects), MIUR (PRIN 2009235JB7). The authors are grateful to Dr. Joop A. Peters for valuable scientific discussions.



Supporting information for this article is available on the WWW under <http://www.angewandte.org> or from the author

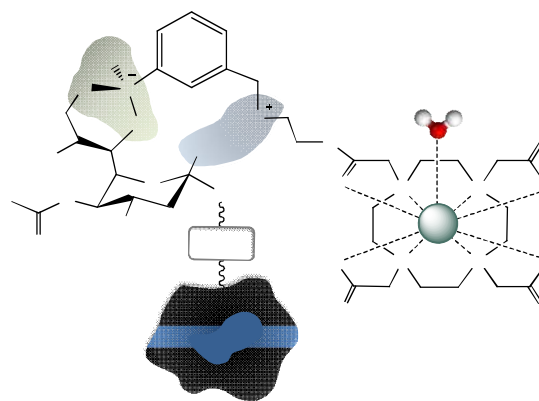


**Figure 1.** Schematic representation of sialic acid recognition by imaging reporter Gd(III)-DOTA-EN-PBA via diol-phenylboronic interaction on the surface of tumor cells.

is based on the reversible formation of five- and six-membered cyclic boronate esters between PBA and the exocyclic polyol function of Sia<sup>[6]</sup> (Scheme 1). Although this type of binding has extensively been exploited for the design of various saccharide sensors<sup>[7]</sup> and Sia determination assays,<sup>[8]</sup> its application for *in vivo* targeting of tumors has not yet been reported. Here, for the first time, we demonstrate *in vivo* visualization of tumors via the highly selective dynamic covalent binding between the diol-function of overexpressed Sia and a PBA-targeting vector conjugated with an MRI reporter (Figure 1).

The DOTA chelate (DOTA = 1,4,7,10-tetraazacyclododecane 1,4,7,10-tetraacetate) has been chosen for the design of the targeting imaging reporter DOTA-EN-PBA due to the superior kinetic stability of its complexes with Ln(III) ions compared to previously reported DTPA-bisamide-PBA-complexes<sup>[5,9]</sup> Conjugation of the PBA-function was carried out via the ethylenediamine (EN) spacer. The aminogroup of DOTA-EN-PBA, being positively charged at physiological pH, facilitates the recognition mechanism through the electrostatic affinity to the negatively charged carboxylic groups of the Sia residues. The role of this auxiliary interaction has been supported previously by a computer modeling study.<sup>[5a]</sup>

Since Sia expression is directly correlated to melanogenesis, the recognition ability of the designed complex has been evaluated on murine melanoma B16-F10 cells. This cell line is commonly used as a well-characterized, highly proliferative tumor model. In melanoma cells, the activity of tyrosinase, the key enzyme for melanogenesis, shows a good correlation with intra- and extracellular Sia levels.<sup>[10]</sup> This indicates an essential role of Sia residues in the enzyme expression and, therefore, in melanoma cells differentiation. Sialylation/desialylation of some relevant molecules, such as melanosomal sialo-glycoconjugates and tyrosinase itself, participate in the regulation of expression of melanogenic functions. For these

reasons, two clones of B16-F10 murine melanoma characterized by a different phenotype, namely melanogenic (B16-F10<sub>m</sub>) and non-melanogenic (B16-F10<sub>non-m</sub>) cells, have been used to test the PBA-based imaging reporter *in vitro*. The two phenotypes have been obtained by growing cells at different pH values. In fact, it is known that B16-F10 cells only form melanin when they are maintained in culture at pH 7.2–7.4.<sup>[11]</sup> At lower pH melanogenesis is inhibited whereas other metabolic processes remain almost unaffected. The level of Sia in the B16-F10<sub>m</sub> clone has been determined to be 3.6 times higher compared to B16-F10<sub>non-m</sub>, which is in accordance with the reported values.<sup>[11]</sup> The specific binding of Gd(III)-DOTA-EN-PBA to the tumor cells overexpressing Sia was assessed by relaxation rates measurements on the washed cell pellets after incubation with a 0.6 mM solution of the complex for 4 hours at 37 °C.

**Table 1.** Response of melanogenic and non-melanogenic cells to the incubation with Gd(III)-DOTA-EN-PBA (0.6 mM, 4h, 37 °C).

| Cell type                | $R_1^{\text{obs}}$ (s <sup>-1</sup> ) | [Gd] (mol/mg protein) <sup>[a]</sup> | [Sia] (mol/mg protein) <sup>[b]</sup> |
|--------------------------|---------------------------------------|--------------------------------------|---------------------------------------|
| B16-F10 <sub>m</sub>     | 0.74 ± 0.03                           | 1.50 (± 0.5) × 10 <sup>-9</sup>      | 7.3 (± 0.6) × 10 <sup>-9</sup>        |
| B16-F10 <sub>non-m</sub> | 0.51 ± 0.04                           | 0.20 (± 0.5) × 10 <sup>-9</sup>      | 1.5 (± 0.4) × 10 <sup>-9</sup>        |

[a] determined by ICP-MS; [b] determined by AbCAM assay. The data represent the results obtained on the basis of five independent experiments.

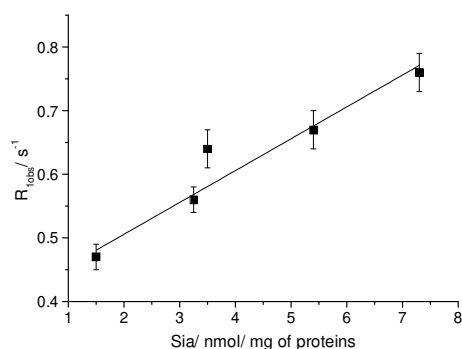


**Figure 2.** Correlation between sialic acid expression and relaxation rates ( $R^2 = 0.9329$ ) measured on cells incubated with Gd(III)-DOTA-EN-PBA. Error bars have been calculated on the basis of three replicate experiments.

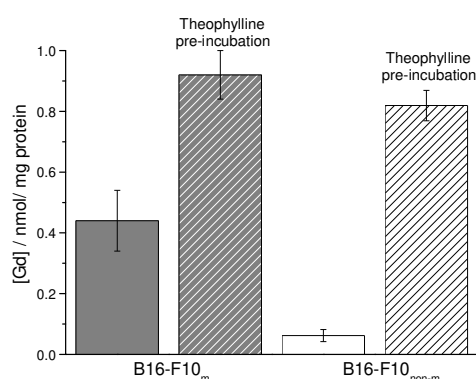


**Figure 3.** Gd-content measured by ICP-MS after incubation of B16-F10<sub>m</sub> (grey solid bar) and B16-F10<sub>non-m</sub> (white solid bar) cells with Gd(III)-DOTA-EN-PBA with or without pre-incubation with theophylline (dashed bars). Error bars have been calculated on the basis of three replicate experiments. Student's *t*-test was used to compare the differences between Gd content before and after theophylline addition.

B16-F10<sub>m</sub>:  $P = 0.0015$ ; B16-F10<sub>non-m</sub>:  $P < 0.0001$ . A  $P$  value  $< 0.05$  has been considered statistically significant.

From the results reported in Table 1 it is evident that there is a marked accumulation of the complex at the melanogenic cells that yields high relaxation rates ( $R_1=1/T_1$ ), as a result of a higher Gd-content, as confirmed by ICP-MS measurements. The relaxation rates are in good correlation with the Sia expression (Figure 2).

In order to get further insights into the relationship between Gd(III)-DOTA-EN-PBA uptake and the sialylation level/melanogenic activity, B16-F10 cells have been incubated for 24 hours with a 0.9 mM solution of theophylline, a well-known pigmentation enhancer in murine melanoma cells.<sup>[11]</sup> As an inhibitor of phosphodiesterase, theophylline has been shown to extensively stimulate pigment production and tyrosinase activity of melanoma cells *in vitro*. As expected, expression of Sia by the cells pre-incubated with theophylline increased significantly, resulting in accumulation of larger quantities of the Gd-complex (Figure 3). This increased binding effect is especially remarkable for the non-melanogenic cells, which is 7 times higher compared to the melanogenic cell, resulting in a similar level of Sia expression for both cell types. The differences in the Gd-levels, measured in this experiment compared to the one reported in Table 1 can be explained by the variability of the Sia-expression by the B16-F10 cells depending on the conditions, i.e. pH, composition of medium, number of passages after cell de-freezing etc.

It is reasonable to assume that successful *in vivo* tumor targeting, based on the recognition of Sia residues by a PBA-vector, could be hampered by its competitive binding to glucose in blood (typically present in between 3.5 and 5.8 mM concentration). The formation of cyclic esters of PBA and glucose is well documented,<sup>[12]</sup> and therefore, the interaction of Gd(III)-DOTA-EN-PBA with B16-F10<sub>m</sub> cells was evaluated at different concentrations in the presence (5.8 mM) or in the absence of glucose. In both cases, the cells were incubated for 4h with the complex after which the incubation medium was removed, the cells were washed, detached with EDTA, and the water proton relaxation rates of cell suspensions were measured.

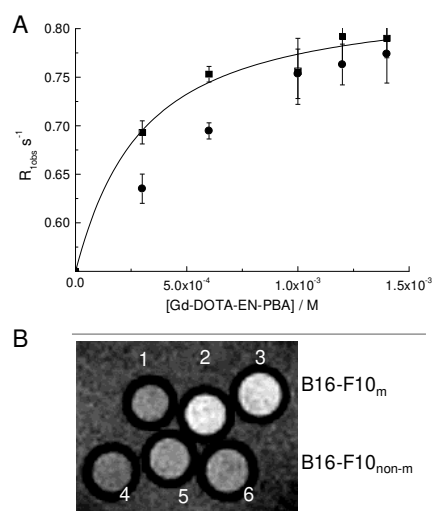


**Figure 4.** (A) Relaxation rates measured for B16-F10 murine melanoma cells, incubated for 4 hours at 37 °C, with various concentrations of Gd(III)-DOTA-EN-PBA in the presence (circles) or the absence (squares) of glucose (5.8 mM), detachment by EDTA has been applied; The continuous line is the result of the fitting of the data by the equations described in the supporting information session . (B)  $T_1$ -weighted spin-echo MR images of agar phantoms containing:

unlabeled cells (1,4), cells incubated with 0.6 mM Gd(III)-DOTA-EN-PBA in the absence (2,4) or in the presence (3,6) of 5.5 mM glucose.

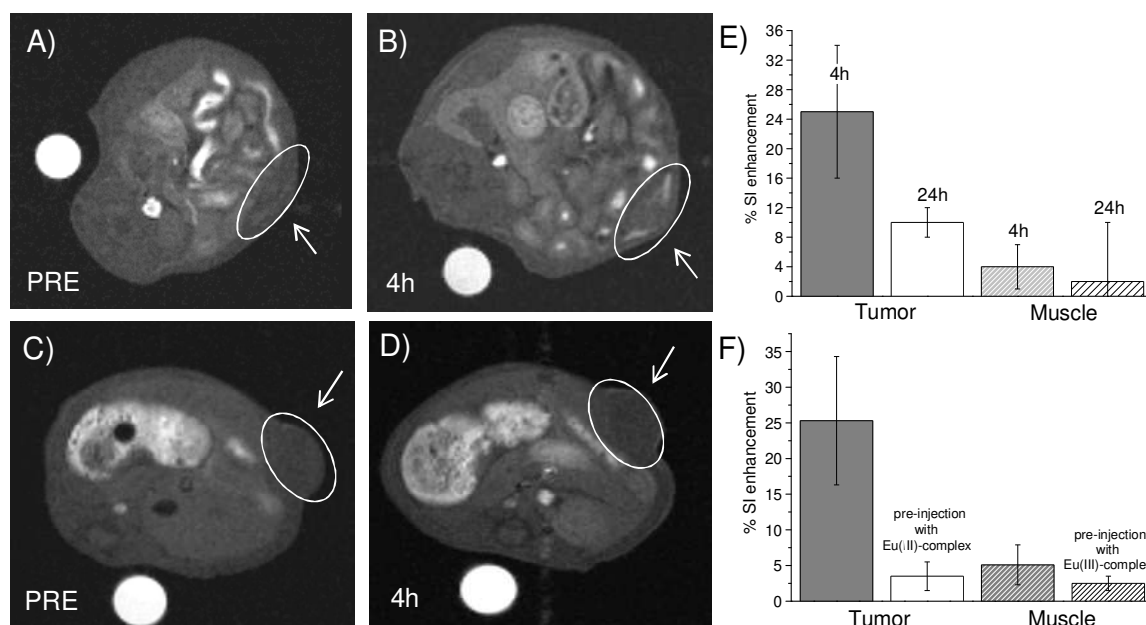


**Figure 5.** Fat-suppressed  $T_1$ -weighted MR spin-echo images of C57BL/6 mice grafted subcutaneously with B16-F10 melanoma cells recorded at 7T (A) before and (B) 4h after the administration of Gd(III)-DOTA-EN-PBA. For comparison, the analogous measurements were performed (C) before and (D) 4h after the administration of Gd-HPDO3A. The corresponding MRI % SI enhancements (E) were measured in melanoma tumors and muscle 4 and 24h after the injection of Gd(III)-DOTA-EN-PBA; the data obtained after injection of Gd(III)-HPDO3A is reported in the Supporting Information (Figure S1). (F) A plot of MRI % SI enhancements measured in melanoma tumors and muscle with or without the PRE-injection with a high dose (0.15mmol/kg) of Eu(III)-DOTA-EN-PBA

As expected, a moderate decrease of relaxation rates as a result of the competitive binding between the complex and glucose in the medium has been observed. However, when the incubation is performed using Gd(III)-DOTA-EN-PBA > 1mM, the competition effect is negligible. At these concentrations the amount of the free (not bound to glucose) complex is high enough to saturate all Sia-residues available on the cell surface as demonstrated by the saturating behavior of the curve. This observation can be rationalized by the lower affinity of PBA to glucose compared to Sia.<sup>[13]</sup> This is due to the fact that D(+)-glucose is present in solution predominantly (>99%) in its pyranose anomeric form. In this configuration, the diol-groups are in an unfavorable position for the formation of PBA-esters compared to those of Sia, positioned on a flexible glycerol tail.<sup>[6]</sup> The analysis of the relaxation rate behavior in the absence of glucose as a function of the concentration of Gd(III)-DOTA-EN-PBA and the equilibria involved are discussed in the Supporting Information. The same minor effect of glucose present in the medium on probe uptake by cells is demonstrated by MRI images of both melanoma clones (Figure 4B). Melanogenic cells (capillaries 2,3) expressing high levels of Sia on their surfaces appear hyperintense on  $T_1$ -weighted images compared to non-melanogenic cells (capillaries 5,6). When cells were incubated with probe in the presence (capillaries 3,6) or in the absence (capillaries 2,4) of glucose, suspensions containing the same type of cells are almost isointense on the images demonstrated only a minor influence of glucose on the binding of Gd(III)-DOTA-EN-PBA to the cells.

Next, *in vivo* MRI experiments were carried out on mice models bearing a tumor xenograft obtained by subcutaneous injection of ca.  $1 \times 10^6$  B16-F10<sub>m</sub> cells on the right flank. After 8 - 10 days, the tumor volume was between 20 and 40 mm<sup>3</sup>, i.e. well detectable by

MRI. Five animals were then intravenously administered with 0.1 mmol/kg of Gd(III)-DOTA-EN-PBA. A second group of mice (n = 5) received the same dose of Gd-HPDO3A (a commercial MRI agent with unspecific vascular and extravascular distribution) as control. Fat-suppressed  $T_1$ -weighted multislice multiecho MR images were recorded before, 4 and 24 hours after the contrast agent administration (Figure 5). The analysis of Signal Intensity (SI) % enhancement measured on the ROI drawn on the whole tumor regions, was of 25% and 10% at 4 and 24 hours after the injection of the targeting probe, respectively, while no persistent SI was observed for animals injected with the control probe (Supporting Information, Figure S1). From the image 5B, it is apparent that the probe can visualize the heterogeneity of tumor. The % SI enhancement recorded on mice treated with Gd-HPDO3A at the same Gd dose (Figure 5C and E) was markedly lower and without any significant difference between muscle and tumor regions. Then, in order to demonstrate the tumor cell binding specificity of Gd(III)-DOTA-EN-PBA, a competition experiment has been performed with Eu(III)-DOTA-EN-PBA (0.15mmol/kg) that does not influence the SI in  $T_1$ -weighted MR images. Briefly, a group of four mice has been treated with 0.15mmol/kg of Eu(III)-DOTA-EN-PBA and after 3h with 0.1mmol/kg of Gd(III)-DOTA-EN-PBA. Figure 5F shows that % SI enhancements measured 4h after the Gd-complex injection on the ROI drawn on the whole tumor regions were significantly lower than those measured in the absence of the competitor, thus supporting the view of Gd(III)-DOTA-EN-PBA binding specificity.

In conclusion, we have demonstrated for the first time the feasibility of *in vivo* tumor targeting based on the recognition of overexpressed sialic acid by a PBA-based imaging reporter. The herein reported results on murine melanoma tumor may be likely extended to other tumor types, such as breast cancer, known to

exhibit high levels of Sia<sup>[1]</sup> as a function of their metastatic potential. The high expression of Sia on the cell surface (ca.  $1 \times 10^9$ /cell) permits their MRI visualization both *in vitro* and *in vivo* using a low molecular weight Gd-complex. The use of small-sized targeting contrast agents has evident advantages compared to the use of targeting nanoparticles in terms of their i) stability, ii) access to the cellular targets or iii) general toxicity issues. This proof of concept opens new avenues for the design of tumor-specific imaging probes. The prolonged retention of Gd(III)-DOTA-EN-PBA at the tumor site after injection suggests the possibility of using this probe for therapy, provided that a suitable radionuclide is used for labeling of the DOTA-EN-PBA ligand. Research along these lines is currently under our close attention.

Received: ((will be filled in by the editorial staff))  
Published online on ((will be filled in by the editorial staff))

**Keywords:** sialic acid · phenylboronates · molecular recognition · tumor targeting · imaging

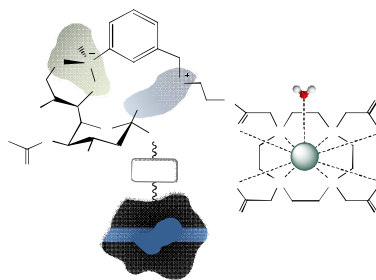
- 
- [1] a) P.-H. Wang, *J. Canc. Mol.* **2005**, *1*(2), 73-81; b) H. Cui, Y. Lin, L. Yue, X. Zhao, J. Liu, *Oncology Reports* **2011**, *25*, 1365-1371.  
[2] a) R. Schauer, *Zoology*, **2004**, *107*, 49-64; b) R. Kannagi, M. Izawa, T. Koike, K. Miyazaki, N. Kimura. *Cancer Sci.* **2004**, *95*, 377-384.  
[3] I.M. Duncker, R. Salinas-Marin, C. Martinez-Duncker, *Int. J. Mol. Imaging.* **2011**, ID 283497.
- 
- [4] a) A. Cazet, S. Julien, M. Bobowski et al. *Carbohydrate Res.* **2010**, *345*, 1377-1383; b) A. Fernandez-Briera, Garzia-Parcerio E. Cuevas, E. Gili-Martin, *Oncology*, **2010**, *78*, 196-204.  
[5] a) K. Djanashvili, G. A. Koning, A. J. G. M. van der Meer, H. T. Wolterbeek, J. A. Peters, *Contrast Media Mol. Imaging*, **2007**, *2*, 35-41; b) K. Djanashvili, T. L. M. ten Hagen, R. Blangé, D. Schipper, J. A. Peters, G. A. Koning, *Bioorg. Med. Chem.* **2011**, *19*, 1123-1130.  
[6] K. Djanashvili, L. Frullano, J. A. Peters, *Chem.-Eur. J.* **2005**, *11*, 4010-4018.  
[7] a) J. Ren, R. Trokowski, S. Zhang, C. R. Malloy, A. D. Sherry, *Magn. Reson. Med.* **2008**, *60*, 1047-1055; b) S. Aime, M. Botta, W. Dastrú, M. Fasano, M. Panero, *Inorg. Chem.* **1993**, *32*, 2068-2071; c) S. Saito, T. L. Massie, T. Maeda, H. Nakazumi, C. L. Colyer, *Sensors*, **2012**, *12*, 5420-5431; d) Z. Guo, I. Shin, J. Yoon, *Chem. Commun.* **2012**, *48*, 5956-5967 (and references therein).  
[8] a) A. Matsumoto, H. Cabral, N. Sato, K. Kataoka, Y. Miyahara, *Angew. Chem. Int. Ed.* **2010**, *49*, 5494-5497; b) S. M. Levonis, M. J. Kiefel, T. A. Houston. *Chem. Commun.* **2009**, 2278-2280.  
[9] C. Cabella, S. Geninatti Crich, D. Corpillo, A. Barge, C. Ghirelli, E. Bruno, V. Lorusso, F. Uggeri, S. Aime, *Contrast Media Mol. Imaging*, **2006**, *1*, 23-29.  
[10] Y. Kinoshita, S. Sato, T. Takeuchi, *Cell Struct. Funct.* **1989**, *14*, 35-43.  
[11] a) D. C. Bennett, *Environ. Health Perspect.* **1989**, *80*, 49-59; b) I. Szabó, S. Geninatti Crich, D. Alberti, F. K. Kálmán, S. Aime. *Chem Commun. (Camb)*. 2012, 28;48(18):2436-8.  
[12] E. Battistini, A. Mortillaro, S. Aime, J.A.. Peters, *Contrast Media Mol. Imaging*, **2007**, *2*, 163-171.  
[13] a) G. Springsteen, B. Wang, *Tetrahedron*, **2002**, 5291-5300; b) M. Regueiro-Figueroa, K. Djanashvili, D. Esteban-Gómez, T. Chauvin, É. Tóth, A. de Blas, T. Rodríguez-Blas, Carlos Platas-Iglesias, *Inorg. Chem.* **2010**, *49*, 4212-4223.
-

## Table of Contents

### Targeting probe

S. Geninatti Crich, D. Alberti, I. Szabo,  
S. Aime, K. Djanashvili\* \_\_\_\_\_  
**Page – Page**

MRI Visualization of Melanoma Cells by  
Targeting Overexpressed Sialic Acid  
with a Gd(III)-DOTA-EN-Phenylboronate  
Imaging Reporter



**Designed to visualize sialic acid expression on tumors:** the novel targeting MRI reporter Gd(III)-DOTA-EN-PBA is shown to be accumulating exclusively at the tumor site after intravenous injection into the murine melanoma B16-F10 mice xenograft. From the MRI Signal Intensity it is possible to quantify sialic acid concentration that is directly associated with tumor malignancy.

# MRI Visualization of Melanoma Cells by Targeting Overexpressed Sialic Acid with a Gd(III)-DOTA-EN-Phenylboronate Imaging Reporter\*\*

*Simonetta Geninatti Crich\*, Diego Alberti, Ibolya Szabo, Silvio Aime, Kristina Djanashvili\**

## SUPPORTING INFORMATION

### Materials and Methods

All chemicals, purchased from Sigma-Aldrich were of analytical grade and were used without further purification. DOTA-EN-PBA was synthesized according to a procedure reported previously,<sup>[1]</sup> and optimized as given below. All the reactions were monitored by TLC on silica plates detecting the components by UV light or by applying the Dragendorff reagent. NMR spectroscopy was performed on Varian Inova-300 spectrometer, operating at 300, 75 and 96 MHz for <sup>1</sup>H, <sup>75</sup>C and <sup>11</sup>B, respectively.

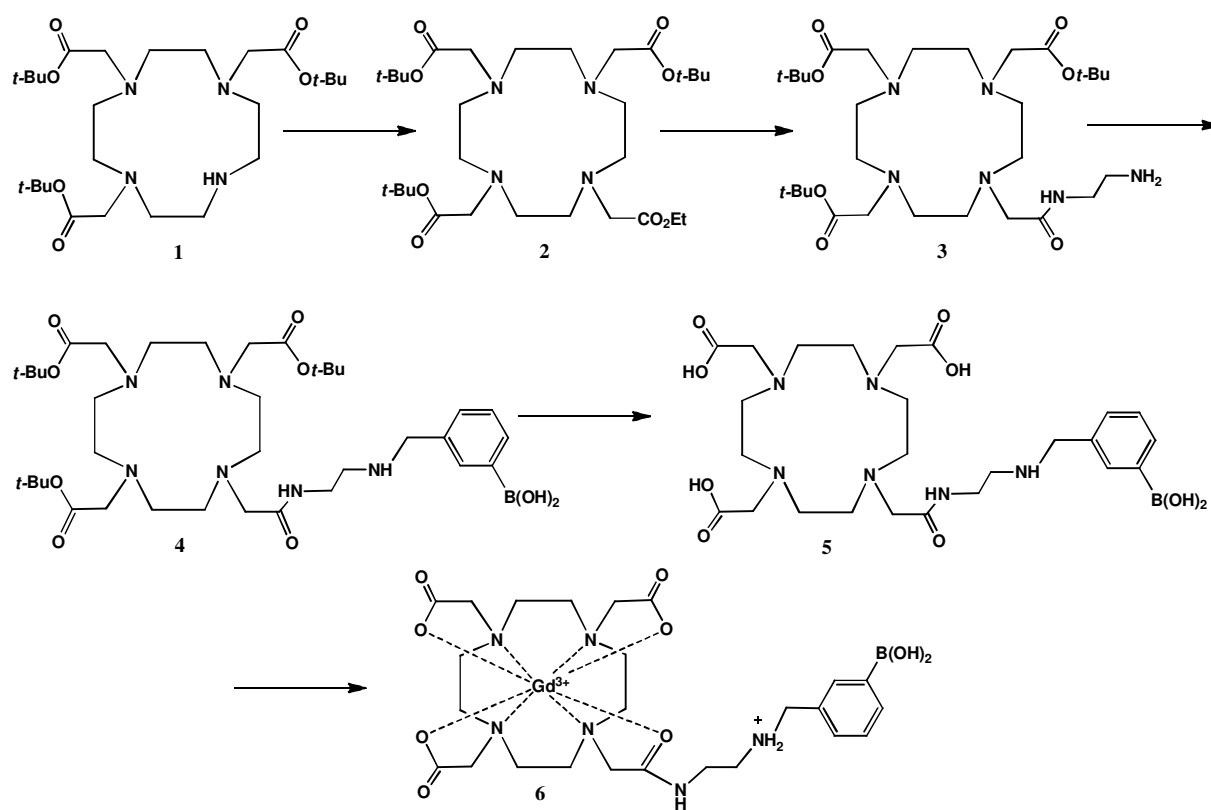
Longitudinal water proton relaxation rate was measured on a Stellar Spinmaster spectrometer (Stellar, Mede, Italy) operating at 20 MHz, by means of the standard inversion-recovery technique (16 experiments, 2 scans). A typical 90° pulse width was 3.5 ms, and the reproducibility of the  $T_1$  data was < 0.5%.

### Cell Lines

Mouse melanoma (B16-F10) cell lines were purchased from the American Type Culture Corporation. Melanogenic B16-F10m cells were obtained by growing cells in standard DMEM (Lonza) medium supplemented with sodium bicarbonate, and glutamine. The cells were incubated at 37 °C in a humidified atmosphere of 5% CO<sub>2</sub>. Non-melanogenic B16-F10<sub>non-m</sub> cells were obtained by growing B16-F10 in RPMI (Lonza) containing sodium bicarbonate and glutamine. The cells were incubated at 37 °C in a humidified atmosphere of 10% CO<sub>2</sub>. Both media were supplemented with 10% (v/v) FBS, 2 mM glutamine, 100 U/ml penicillin, and 100 U/ml streptomycin. Melanogenesis was evaluated by measuring the absorbance of cell lysate and medium (dissolved in NaOH 1M) at 490 nm observing its linear dependency on the number of cell passages. The Sia expression on B16-F10 cells was determined using a commercially available AbCAM assay.



## Synthesis



**Scheme S1.** Synthetic route for the preparation of Gd(III)-DOTA-EN-PBA.

**Tris-1,4,7-*tert*-butoxycarbonylmethyl-10-ethoxycarbonyl-1,4,7,10-tetraaza-cyclododecane (2):** Solid K<sub>2</sub>CO<sub>3</sub> (3.15 g, 22.77 mmol) was added to a solution of the HBr salt of tris-1,4,7-*tert*-butoxycarbonylmethyl-1,4,7,10-tetraazacyclododecane (**1**) (2.03 g, 3.36 mmol) in 28 mL of acetonitrile, and then the mixture was stirred for 1 h at room temperature. The suspension was cooled down to 0 °C in an ice-water bath and a solution of ethyl bromoacetate (0.63 g, 3.78 mmol) in 5 mL of acetonitrile was added dropwise over 15 min. The reaction mixture was stirred overnight at ambient temperature. The suspended salts were removed by filtration and the solvent was evaporated under reduced pressure. After purification of the residue by column chromatography (silica, CH<sub>2</sub>Cl<sub>2</sub>/MeOH gradient from 95:5 to 80:20) 2.63 g (88%) of **2** were obtained.

<sup>1</sup>H NMR (CDCl<sub>3</sub>, 25 °C, TMS): δ = 1.16 (t, *J* = 7.2 Hz, 3H), 1.45 (s, 18H), 1.47 (s, 9H), 1.80–3.80 (broad multiplets, 24H), 4.17 (q, *J* = 7.2 Hz, 2H). <sup>13</sup>C NMR (CDCl<sub>3</sub>, 25 °C, TMS): δ = 14.14, 30.95, 27.91, 28.02, 51.96, 53.50, 54.71, 54.91, 55.67, 55.73, 62.26, 82.08, 82.16, 172.92, 173.02, 173.60.

**Monoamide of ethylenediamine and tris-1,4,7-*tert*-butoxycarbonylmethyl-10-carboxymethyl-1,4,7,10-tetraazacyclododecane (3):** This compound was prepared and characterized according to a published procedure<sup>[2]</sup> in 72% yield (1.53 g).

**Conjugate of 3 and 3-formylphenylboronic acid (4):** To a solution of **3** (1.34 g, 2.18 mmol) in 15 mL of methanol, 3-formylphenylboronic acid (0.35 g, 2.39 mmol) was added. After addition of 5 mL of freshly distilled triethylamine, the reaction mixture was stirred for 2 h at room temperature. After the conversion of the amine to the imine (followed by NMR), NaBH<sub>4</sub> (139 g, 26.41 mmol) was carefully added to the reaction mixture. The resulting solution was stirred at room temperature for 12 h. The solvent was removed under reduced pressure to give a brownish foam. The residue was taken up in water and the resulting mixture was extracted three times with dichloromethane. After evaporation of the combined organic phases, 1.56 g of compound **4** (97%) were obtained, which was used in the next reaction step without further purification.

**Deprotection of 4.** A solution containing **4** (2.34 g, 3.13 mmol) in 5 mL CH<sub>2</sub>Cl<sub>2</sub>/TFA (3:1) was stirred overnight. The solvent was removed under reduced pressure; the residue was taken up in methanol several times, which was removed each time by evaporation, until a light yellow foam was formed. The final residue was dissolved in water and the pH was adjusted to 12. This basic solution was brought on the ion exchange column and rinsed with water until the pH of the eluent was neutral. The final product was eluted with a mixture of pyridine (10% in water)/ethanol (1:1). The fractions obtained were analyzed by TLC. Lyophilization of the purified material gave 615 mg (1.06 mmol, 33%) of **5**.

<sup>1</sup>H NMR (D<sub>2</sub>O, 25 °C, pH 12, internal reference *t*-BuOH at 1.20 ppm): δ = 2.78–3.48 (m, 20H), 3.68–3.71 (m, 8H), 4.70 (s, 2H), 7.49–7.73 (m, 4H).

<sup>13</sup>C NMR (75 MHz, D<sub>2</sub>O, 25 °C, pH 12, internal reference *t*-BuOH at 31.20 ppm): δ = 35.98, 46.59, 48.66, 48.94, 50.64, 51.04, 51.23, 52.23, 56.70, 57.12, 128.96, 130.60, 132.66, 134.91, 135.42, 137.85, 169.81, 173.06, 178.46.

<sup>11</sup>B NMR (D<sub>2</sub>O, 25 °C, pH 12, external reference 0.1M H<sub>3</sub>BO<sub>3</sub> at 0 ppm): δ = –16.79.

The complexation of the ligand with Gd(III)-ion was performed by the dropwise addition of an aqueous solution of GdCl<sub>3</sub> to an aqueous solution of DOTA-EN-PBA (5% excess). The mixture was stirred at 50 °C for 24 hours, and the pH was adjusted to 7.4 using a 1M solution of NaOH, and maintained constant until no changes due to the complexation were observed. The final Gd(III)-DOTA-EN-PBA complex was obtained as a white powder after lyophilization. The formation of the complex was identified by ESI-MS: *m/z* = 735.30. The absence of free Gd(III) ion was confirmed by a xylenol orange test.<sup>[2]</sup>

[1] K. Djanashvili, T. L. M. ten Hagen, R. Blangé, D. Schipper, J. A. Peters, G. A. Koning, *Bioorg. Med. Chem.* 2011, 19, 1123-1130.

[2] J. P. André, C. F. G. C. Geraldés, J. A. Martins, A. E. Merbach, M. I. M. Prata, A. C. Santos, J.J.P. de Lima, E. Tóth. *Chem. Eur. J.* 2004, 10, 5804.

[3] A. Barge, G. Gravoto, E. Gianolio, F. Fedelil. *Contrast Med. Mol. Imaging.* 2006, 1, 184.

## MRI

MR images were acquired on a Bruker Avance 300 spectrometer (7T) equipped with a Micro 2.5 microimaging probe. The system is equipped with two birdcage resonators with 30 and 10mm inner diameter, respectively. Glass capillaries containing about  $2 \times 10^6$  cells were placed in an agar phantom and MR imaging was performed by using a standard  $T_1$ -weighted multislice spin-echo sequence (TR/TE/NEX=200/3.3/8, Matrix size = 128 x 128, FOV = field of view: FOV = 1.2 cm (cell images), FOV = 2.8 cm (mice images), NEX = number of excitations).

The  $T_1$  relaxation times were calculated using a standard saturation recovery spin echo. For in vivo MRI, the animals were anesthetized before examination by injecting tiletamine/zolazepam (20 mg/kg; Zoletil 100, Virbac, Milan, Italy) and xylazine (5 mg/kg; Rompun, Bayer, Milan, Italy). Mice of group 1 (n = 4) received intravenously 0.1 mmol/kg of Gd(III)-DOTA-EN-PBA, and mice of group 2 (n = 4) received the same amount of Gd-HPDO3A (Prophance, Bracco, Italy). MR images were acquired before 4, and 24 h after the contrast agent administration using a  $T_1$ -weighted, fat-suppressed, multislice protocol (TR/TE/NEX 250/3.2/6, 1 slice, 1 mm). Fat suppression was performed by applying a pre-saturation pulse ( $90^\circ$  BW = 1400 Hz) at the absorption frequency of fat (-1100 Hz from water). The mean signal intensity (SI) values were calculated in the regions of interest (ROI) manually drawn on the whole tumor. The measured SI was normalized to a standard Gd(III) solution to take into account differences in the absolute SI values among different images obtained after mouse repositioning in the MRI scanners. The normalization was carried out by dividing the  $SI_0$  values of the ROI drawn on the tumor to the SI values of the ROI drawn inside the reference tube ( $SI_{ref}$ ):

$$SI \text{ normalized } (SI_n) = SI_0 / SI_{ref}$$

The mean measured SI was normalized by using a standard solution of Gd in 1%  $HNO_3$ . The mean SI enhancement (%) of target tissues (TT) was calculated according to the following equation:

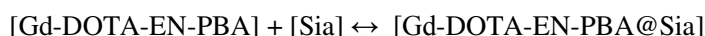
$$SI \text{ \% Enhancement} = ((\text{mean SI (TT) post-contrast}) - (\text{mean } SI_n \text{ (TT) pre contrast})) / (\text{mean } SI_n \text{ (TT) pre-contrast}) \times 100.$$

Tumor region has been defined from  $T_2$  weighted RARE images recorded before the acquisition of each  $T_1$ -weighted spin-echo image. As a consequence of their longer  $T_2$ , tumors appear hyperintense with

respect normal tissues. Due to the long time analysis (up to 24 hours) the reposition the animals was unavoidable, making it impossible to compare images slice by slice. Therefore, the SI enhancement has been calculated on the whole tumor by averaging SI enhancement measured on each slice.

### Analysis of the relaxation rate behavior (Figure 4A) measured in the absence of glucose as function of Gd(III)-DOTA-EN-PBA concentration.

The following equilibria have been considered for the analysis:



$$K_a = [\text{Gd-DOTA-EN-PBA@Sia}] / ([\text{Sia}]_f \times [\text{Gd-DOTA-EN-PBA}]_f)$$

$$[\text{Gd-DOTA-EN-PBA}]_{\text{tot}} = [\text{Gd-DOTA-EN-PBA@Sia}] + [\text{Gd-DOTA-EN-PBA}]_f$$

Where,  $[\text{Sia}]_t$  = Sialic acid concentration on B16-F10 cells determined by AbCAM assay

$[\text{Gd-DOTA-EN-PBA}]_{\text{tot}}$  = the total amount of complex added to the cell media

$[\text{Gd-DOTA-EN-PBA}]_f$  = the free complex concentration.

$$[\text{Sia}]_t = [\text{Gd-DOTA-EN-PBA@Sia}] + [\text{Sia}]_f$$

$R_{\text{obs}}$  = observed relaxation rate measured on cell pellets after incubation with increasing complex concentrations.

$R_{\text{ld}}$  = Diamagnetic contribution to the observed relaxation rate measured on untreated cells without incubation with Gd- DOTA-EN-PBA.

Using equation  $R_{\text{obs}} = R_{\text{ld}} + r_{1p}^b \times [\text{Gd-DOTA-EN-PBA@Sia}]$  it was possible to estimate an association constant of  $3700 \text{ M}^{-1}$  and an  $r_{1p}^b$  of  $4 \text{ mM}^{-1}\text{s}^{-1}$  (at 7T).

**Table S1.** Signal intensity enhancement (%) measured on kidneys, liver and spleen 4 and 24h after injection of Gd-complexes.<sup>[a]</sup>

| Gd-complex/ time          | Kidneys | Liver | Spleen  |
|---------------------------|---------|-------|---------|
| <b>Gd-DOTA-EN-PBA/4h</b>  | 39 ± 10 | 5 ± 3 | 2 ± 1   |
| <b>Gd-DOTA-EN-PBA/24h</b> | 15 ± 3  | 2 ± 1 | 0.5 ± 1 |
| <b>Gd-HPDO3A/4h</b>       | 31 ± 5  | 1 ± 1 | 0.5 ± 1 |
| <b>Gd-HPDO3A/24h</b>      | 5 ± 3   | 1 ± 1 | 1 ± 1   |

[a] The stomach and intestines are highlighted before and after the injection of the contrast agents because the food provided to the mice contains paramagnetic ions (such as  $\text{Fe}^{3+}$  and  $\text{Mn}^{2+}$ ). The effect of the diet on the appearance of hyperintensity in regions of gastrointestinal tract is well known. Only kidneys show a specific enhancement due to the elimination of the Gd-containing complex through this organ.

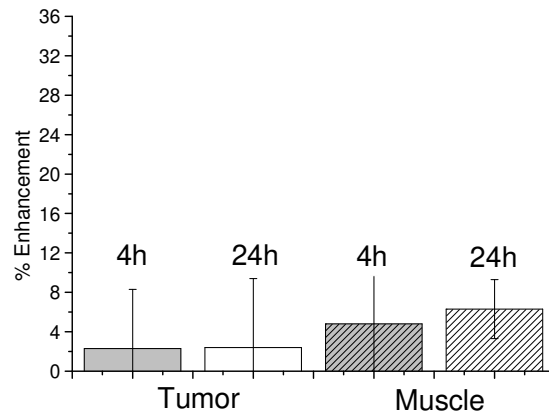


**Figure S1** A plot of MRI SI enhancements (%) measured in melanoma tumors and muscle 4 hours after the injection of Gd(III)-HPDO3A. Student's t-test was used to compare the differences between SI measured in the presence and in the absence of Eu(III)-complex, tumors:  $P = 0.01$ ; muscles:  $P=0.07$  (not significant).

### Monitoring of melanogenesis process on B17-F10 cell line

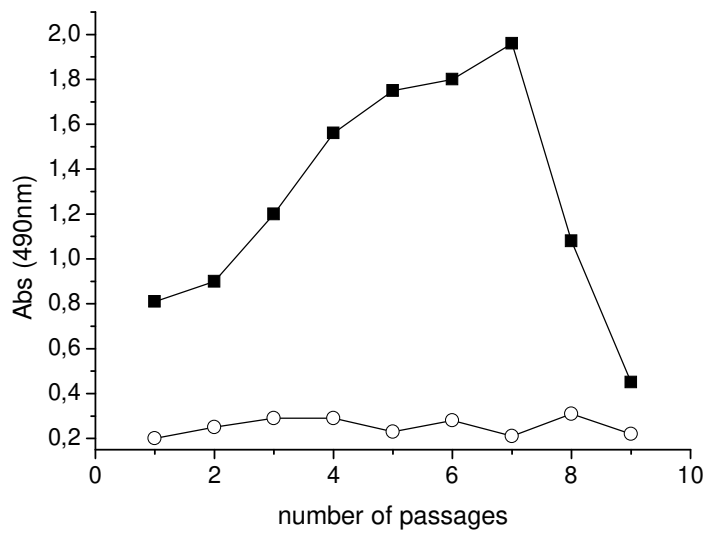


**Figure S2.** Cell lysate absorbance dependence on the number of detaching cell passages. Cells lysates were obtained by dissolving cells in NaOH (0.1M) and absorbance was measured at 490 nm.

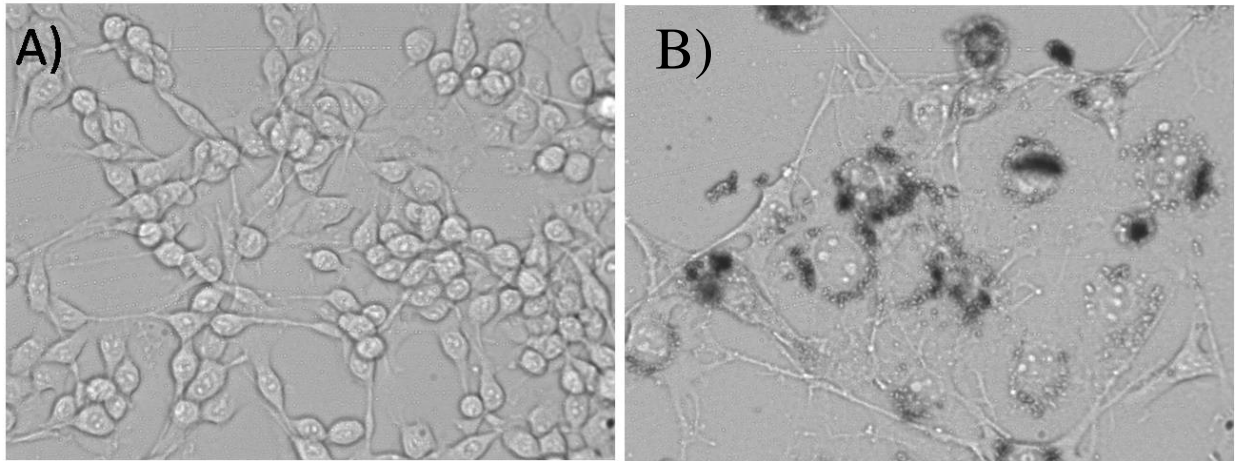


**Figure S3.** Light microscope photographs (20x) of non-melanogenic (A) and melanogenic (B) B16-F10 cells.